

## CAMS Service Evolution



CAMAERA

### D3.1 Implementation and verification of M7 modal scheme into operational IFS cycle

Due date of deliverable	30 June 2025
Submission date	30 June 2025
File Name	CAMAERA-D3.1-V1.1
Work Package /Task	WP3/T3.1
Organisation Responsible of Deliverable	KNMI
Author names	Vincent Huijnen, Ramiro Checa-Garcia, Lianghai Wu, Philippe Le Sager, Thanos Tsikerdekis, Twan van Noije, Tommi Bergman, Swen Metzger, Samuel Remy
Revision number	1.1
Status	
Dissemination Level	Public



Funded by the  
European Union

The CAMAERA project (grant agreement No 101134927) is funded by the European Union.

Views and opinions expressed are however those of the author(s) only and do not necessarily reflect those of the European Union or the Commission. Neither the European Union nor the granting authority can be held responsible for them.

## 1 Executive Summary

As part of the CAMS AERosol Advancement (CAMAERA) project a large investment is made to implement an alternative module for aerosol microphysics in the global model component in support of CAMS. In this way, CAMAERA may in future enhance the quality of key products of the CAMS service. For this, we have implemented a modal aerosol module based on M7 (Vignati et al., 2004) and HAMM7 as described in Tegen et al. (2019) into the IFS, as an alternative of the default IFS-AER scheme. Here we describe a first technical implementation of the HAMM7 aerosols module into CY49R1 of the IFS.

We present short simulations of the new HAMM7 module describing aerosol emissions, transport, microphysical conversion, dry and wet deposition, and sedimentation, for the aerosol tracers which represent sea salt, desert dust, sulphate, organic matter and black carbon. We diagnosed the distribution of aerosol burden, its tendencies, and the optical properties through Aerosol Optical Depth (AOD), its absorbing component (AAOD) and the mass extinction coefficient (MEC). In particular, we compared two configurations of IFS-HAMM7, which differed in their specification of emissions, and compared this to a default configuration of IFS-AER.

While both IFS-HAMM7 versions show correct reproduction of the spatial distribution of the aerosol types, the version with enhanced emissions shows the best performance, although overall still significantly lower aerosol burdens than IFS-AER. Even though we have not yet used actual observations to validate this configuration, this strongly suggests that the AOD in IFS-HAMM7 is still on the low side. One of the key reasons appears to be a more efficient removal of aerosols due to wet deposition in IFS-HAMM7 compared to IFS-AER. During the second phase of the CAMAERA project we will put efforts towards a more stable code base, along with improvements on the physical parameterization of the module, in order to reach similar or better performance compared to IFS-AER with respect to main aerosol quantities.

## Table of Contents

1	Executive Summary .....	3
2	Introduction .....	5
2.1	Background.....	5
2.2	Scope of this deliverable .....	5
2.2.1	Objectives of this deliverable .....	5
2.2.2	Work performed in this deliverable.....	6
2.2.3	Deviations and counter measures.....	6
2.2.4	CAMAERA Project Partners.....	6
3	Implementation .....	8
3.1	IFS.....	8
3.1.1	ifs-source.....	9
3.1.2	ifs-scripts and input data .....	10
3.1.3	ifs-test.....	12
3.1.4	ifs-defaults .....	12
3.2	OpenIFS .....	12
4	Description of the HAMM7 modules .....	13
4.1	Microphysical core .....	13
4.2	Aerosol emissions.....	14
4.3	Aerosol removal processes.....	14
4.4	Aerosol optical properties.....	15
5	Verification .....	16
5.1	Comparison of total columns.....	17
5.2	Mass diagnostics .....	20
5.3	Comparison of AOD.....	23
6	Conclusion .....	25
	References .....	26

## 2 Introduction

### 2.1 Background

The European Union's flagship Space programme Copernicus provides a key service to the European society, turning investments in space-infrastructure into high-quality information products. The Copernicus Atmosphere Monitoring Service (CAMS, <https://atmosphere.copernicus.eu>) exploits the information content of Earth-Observation data to monitor the composition of the atmosphere. By combining satellite observations with numerical modelling by means of data assimilation and inversion techniques, CAMS provides in near-real time a wealth of information to answer questions related to air quality, climate change and air pollution and its mitigation, energy, agriculture, etc. CAMS provides both global atmospheric composition products, using the Integrated Forecasting System (IFS) of ECMWF - hereafter denoted the global production system -, and regional European products, provided by an ensemble of eleven regional models - the regional production system.

The CAMS AERosol Advancement (CAMAERA) project will provide strong improvements of the aerosol modelling capabilities of the regional and global systems, on the assimilation of new sources of data, and on a better representation of secondary aerosols and their precursor gases. In this way CAMAERA will enhance the quality of key products of the CAMS service and therefore help CAMS to better respond to user needs such as air pollutant monitoring, along with the fulfilment of sustainable development goals. To achieve this purpose CAMAERA will develop new prototype service elements of CAMS, beyond the current state-of-art. It will do so in very close collaboration with the CAMS service providers, as well as other tier-3 projects. In particular, CAMAERA will complement research topics addressed in the CAMEO project, which focuses on the preparation for novel satellite data, improvements of the data assimilation and inversion capabilities of the CAMS production system, and the provision of uncertainty information of CAMS products.

### 2.2 Scope of this deliverable

#### 2.2.1 Objectives of this deliverable

The aerosol module in the current global analysis and forecast system in the IFS cycle 49R1, IFS-AER (Rémy et al., 2022; 2024; Metzger et al. 2024), is based on a bin-bulk representation of tropospheric aerosol, with an extension towards stratospheric aerosols. While it is very successful to provide key aerosol air quality information, such as PM<sub>2.5</sub> and PM<sub>10</sub>, along with analyses and forecasts of AOD in the operational context in CAMS, it provides only limited information on the particle size distribution. Moreover, IFS-AER does not account for internal mixing of different chemical components, which has important implications for the way the aerosol optical properties and aerosol-cloud interactions (droplet activation and removal of aerosols by clouds and precipitation) can be described. This impacts the life cycle of the aerosol particles and their direct and indirect radiative effects.

Here we address these fundamental limitations by the introduction of a modal scheme based on M7 (Vignati et al., 2004; Tegen et al., 2019) into the IFS. Modal schemes are designed to enable the parameterization of processes like cloud droplet activation (Abdul-Razzak and Ghan, 2000; Morales Betancourt and Nenes, 2014) and in- and below-cloud scavenging (Croft et al., 2009; Croft et al., 2010) by representing aerosol sizes in an efficient way using lognormal distributions.

The implementation reported here required the selection of relevant code, the preparation of interfaces, as well as the preparation of test configuration, emission input data, and preparation of diagnostics to allow assessment of the performance.

We also established a coupling of secondary inorganic aerosol with precursor gases through the use of the EQSAM4Clim scheme (Metzger et al., 2018), as reported in a separate Deliverable (D3.2). This requires a careful coupling of aerosol precursor gases and mineral cations with individual aerosol types as represented in M7.

### 2.2.2 Work performed in this deliverable

In this deliverable the work as planned in the Description of Action (DoA, WP3 T3.1) was performed:

**Task 3.1:** Implementation of modal aerosol model into recent IFS cycle: Porting of M7 from OpenIFS 43R3 to a recent IFS cycle; Verify model performance against existing reference model versions

### 2.2.3 Deviations and counter measures

No deviations have been encountered.

### 2.2.4 CAMAERA Project Partners

HYGEOS	HYGEOS SARL
ECMWF	EUROPEAN CENTRE FOR MEDIUM-RANGE WEATHER FORECASTS
Met Norway	METEOROLOGISK INSTITUTT
RC.io	RESEARCHCONCEPTS IO
BSC	BARCELONA SUPERCOMPUTING CENTER-CENTRO NACIONAL DE SUPERCOMPUTACION
KNMI	KONINKLIJK NEDERLANDS METEOROLOGISCH INSTITUUT-KNMI
SMHI	SVERIGES METEOROLOGISKA OCH HYDROLOGISKA INSTITUT
FMI	ILMATIETEEN LAITOS
MF	METEO-FRANCE
TNO	NEDERLANDSE ORGANISATIE VOOR TOEGEPAST NATUURWETENSCHAPPELIJK ONDERZOEK TNO
INERIS	INSTITUT NATIONAL DE L ENVIRONNEMENT INDUSTRIEL ET DES RISQUES - INERIS
IOS-PIB	INSTYTUT OCHRONY SRODOWISKA - PANSTWOWY INSTYTUT BADAWCZY

## CAMAERA

FZJ	FORSCHUNGSZENTRUM JULICH GMBH
AU	AARHUS UNIVERSITET
ENEA	AGENZIA NAZIONALE PER LE NUOVE TECNOLOGIE, L'ENERGIA E LO SVILUPPO ECONOMICO SOSTENIBILE

### 3 Implementation

The Integrated Forecasting System (IFS) is an ecosystem of different types of code, scripts and data. The IFS is built and maintained to work on ECMWF's High Performance Computing (HPC) infrastructure and is used to provide forecasts of meteorological and related quantities. As part of the CAMS global operational service, a version of IFS is maintained, which contains modules to describe gas-phase and aerosol aspects. Gas-phase chemistry is based on a modified version of the CB05 tropospheric chemistry, coupled with BASCOE-based chemistry in the stratosphere, while the aerosol module is based on the AER scheme, see ECMWF (2024) for further information. The AER scheme, in its default configuration, contains tracers for sulphate, ammonium, nitrate, hydrophilic and hydrophobic black carbon and organic matter, secondary organic aerosol, sea salt and mineral dust. Three bins are used for sea salt and dust, while the other components are simulated by a single tracer representing the total mass (or number of particles). In AER, the different aerosol components are externally mixed.

The modal aerosol scheme that is considered here is based on the Hamburg Aerosol Model version 2.3 (HAM2.3; Tegen et al., 2019), which includes the M7 microphysical core (Vignati et al., 2004). In the remainder of this report we refer to this module as 'HAMM7'. Different to the AER module, in HAMM7 sulphate, black carbon, organic matter, sea salt and mineral dust are described using seven lognormal modes, with internal mixing within the modes. At the start of this project activities were ongoing to introduce this module in OpenIFS 48r1, as reported in van Noije et al. (2025). This constitutes an update of the activation of the atmospheric composition modules in OpenIFS 43r3 (Huijnen et al., 2022).

In the following sections we describe the changes made to enable the activation of the HAMM7 module into the respective code and script environments that come with IFS CY49R1. First, we focus on the constituents of the IFS model, and then continue with further details, along with comments on specific differences with respect to the OpenIFS implementation.

#### 3.1 IFS

Our initial implementation of HAMM7 was prepared in cycle CY49R1.1 of the IFS. Here we start off from branch `nk9_CY49R1.1_GHG_rean_v0`. Compared to the IFS reference branch (CY49R1.1) this experimental branch contains some of the developments that are planned for inclusion in CY50R1. In Table 1 we provide an overview of the associated repositories of IFS. We indicate, which of them we provide and in which of them we performed changes. Note that the core of the implementation is done in `ifs-source`. On the other hand, `ifs-scidoc` is not provided as the documentation will only be prepared once we have a fully functional and validated implementation.

**Table 1.** Overview of repositories as part of the IFS CY49R1 and changed associated to the HAMM7 implementation.

Repository	Description	Changes	Provided
<code>ifs-bundle.git</code>	Build-system for IFS - <code>ecbuild</code>	No	Yes
<code>ifs-source.git</code>	Core Fortran source code (including a few files in C/C++)	Yes (arpifs)	Yes
<code>ifs-scripts.git</code>	Korn shell scripts and SMS/ <code>ecFlow</code> suite definitions	Yes	Yes
<code>ifs-suites.git</code>	Python software for creating <code>ecFlow</code> suites	No	Yes
<code>ifs-scidoc.git</code>	LaTeX scientific documentation	No	No

ifs-defaults.git	PrepIFS defaults files	Yes	Yes
ifs-test.git	CI testing system	Yes	Yes

### 3.1.1 ifs-source

The development began with the above mentioned nk9\_CY49R1.1\_GHG\_rean\_v0 and a version of OpenIFS cy48r1 with a preliminary implementation of HAMM7. However, rather than a direct full integration of both codes, we proceed initially defining a set of steps to reduce the complexity of our validation in each step of the implementation.

- a.** Introduce new tracers
- b.** Introduce emissions by sectors
- c.** Introduce online emissions driven by wind (dust and sea-salt)
- d.** Introduce removal processes
- e.** Introduce aerosol conversion
- f.** Introduce module for aerosol optics
- g.** Include the interaction with radiation
- h.** Evaluate/add heterogeneous chemistry and aerosols-cloud interactions

The information of the tracers added when using HAMM7 is detailed in specific text-table files where information needed for ifs-scripts is provided to generate a consistent name-list of aerosols tracers as explained in section 3.1.2.

The HAMM7 code is implemented essentially as an alternative option to the default AER scheme. This is done in a manner as least intrusive as possible. The interface towards specific processes in AER scheme has an equivalent in HAMM7. In the Table 2 we show an overview of these equivalences.

**Table 2.** Overview of equivalent interface routines between AER and HAMM7

AER	HAMM7	Purpose and comments
phys_ec/aer_phy2.F90	m7/m7_phy2.F90	Interface to surface processes
phys_ec/aer_src.F90	m7/m7_src.F90	Interface to emission parameterization
phys_ec/aer_phy3.F90	m7/hamm7_interface.F90	Aerosol conversion in atmosphere, and diagnostics. Routines called through aer_phy3_layer.F90
phys_ec/aer_dustemis.F90	m7/m7_src_dust.F90	Mineral dust emissions
phys_ec/aer_ssalt[_xx].F90	m7/m7_src_ss.F90	Sea-Salt emissions

Initialization of the HAMM7 coding aspects is governed through the routine HAMM7\_INIT, as called through control/cnt4.F90.

Routine HAMM7\_INTERFACE is the largest and most important interface routine and currently contains calls to the HAMM7-related routines with purposes as indicated in Table 3.

The order of the various processes is as indicated. The aerosol tracer fields are updated after each process, which forms the input to the next process. For instance, the optics is computed at the end, which includes the impact of any of the preceding processes.

Also, after each process a check is done to ensure non-negative tracer mass, see routine `xt_borrow`. This routine conserves tracer mass and re-distributes it in the vertical dimension, if necessary.

Also, across each physical process a global budget accounting is invoked to keep track of the global mass conversion due to individual processes. This is handled in routines `FILL_ZTEND` and `CHEM_INEXT`, and governed by the overall switch `LCHEM_DIA`.

**Table 3.** Overview of processes and corresponding subroutines handled through routine `HAMM7_INTERFACE`.

Process	subroutine	Purpose and comments
1. Initialization	<code>tm5m7_init</code> and <code>hamm7_init</code>	Ensure proper initial values of several arrays
2. Microphysics	<code>ham_subm_interface</code>	Aerosol microphysics (condensation, coagulation, nucleation, water uptake)
3. Wet deposition	<code>wetdep_interface</code>	Wet removal due to convective and large-scale precipitation
4. Sedimentation	<code>sedi_interface</code>	Sedimentation
5. Dry deposition	<code>drydep_interface</code>	Dry deposition
6. Negatives fixing	<code>chem_negat</code>	Ensure that total tendency does not cause the tracer to get negative
7. Optics	<code>m7_calc_aeropt</code>	Compute optical aspects
8. Fill output arrays	<code>export_to_pgfl</code>	Fill arrays, which are ported outside this routine

### 3.1.2 ifs-scripts and input data

The ifs-scripts repository contains mainly korn shell scripts used to setup the executable and handle the model input and output data. In addition, there is a wide variety of heterogeneous input data and information used to setup and drive the IFS, apart from the meteorological and composition initial and boundary conditions.

Changes to the ifs-script repository to support the HAMM7-module mainly concern script **aero\_setup**. This script handles the main switches to select, which aerosol module to choose, as well as some of the options for parameterization. Specifically, it handles on a high level the list of aerosol tracers involved in the scheme and prepares for the namelist to be read by the IFS, based on various specification files (see Table 4). The key information is contained in a file named: **bins\_hamm7ver1.csv** (bins is inherited from AER scheme naming convention, but it refers to components in HAMM7). In this file 39 tracers are defined as well as their corresponding “type”. The latter is a concept derived from the AER-scheme; it is used to provide consistent subsets of aerosols species that can be used independently.

The emissions in IFS-COMPO are configured in an emissions specification file. As HAMM7 uses a different set of tracers this requires also a full review and modification of the aerosol part of the emissions specification file. Now, mass-flux can be directly emitted into specific components of a mode as far as they represent the mass concentration. Further developments

have been added in the IFS-COMPO code to consistently evaluate the number of particles emitted according to flexible particle size distributions (PSD) following a log-normal shape. Therefore, the emission specification file also needs to indicate for each mass flux the PSD of the emissions that will be used to compute the number of particles emitted into the corresponding mode. The emission specification has been extended to also include the option to specify aspects related to the particle size distribution.

The HAMM7 implementation in the IFS comes with additional datafiles in netcdf-format which are used to compute the aerosol growth due to water uptake, and the optical properties, see also Table 4. Scripts **mklinks** and **model**, which are part of the ifs-scripts repository, require some adaptations to ensure a correct linking of these ancillary datafiles to the actual model experiment.

**Table 4.** Overview of specification files and ancillary datafiles required for the hammm7 implementation

Process	datafile	Purpose and comments
<b>1. Tracer definition</b>	bins_hamm7ver1.csv	Defines the selection of aerosol tracers in the model, and governs the definition of its associated grib numbers
<b>2. Emissions specification</b>	compo_emissions_rean_eac5.ant.v6.2.HAMM7_v1.txt	Specifies the settings for the emissions, to handle the preparation of (grib-based) emission input data and corresponding namelist entries
<b>3. Optics diagnostics</b>	wavelengths_hamm7ver1.csv	Governs the definition of grib numbers for the various AOD output diagnostics at different wavelengths
<b>4. Aerosol hygroscopic growth</b>	lut_kappa.nc	Lookup table of aerosol hygroscopic growth factor required to compute aerosol size distribution.
<b>5. HAMM7 namelist</b>	Namelist.echam	namelist file with HAMM7-related switches
<b>6. Optics information</b>	lut_optical_properties_lw_M7.nc lookup_table.nc refractive_indices_hdfstyle.nc lut_optical_properties_M7.nc	Lookup table, which is used to specify the optical properties of the aerosol

### 3.1.3 ifs-test

We have introduced two tests for HAMM7 specifically, see Table 5. Furthermore, as we need to adapt the code also in shared modules/subroutines, we also validated that all other ifs-tests are passed in our implementation.

**Table 5.** Specification of ifs-tests prepared for HAMM7

Test	Res.	Purpose
<b>compo_fc_climrad_m7</b>	T21	Equivalent of compo_fc_climrad for HAMM7
<b>compo_fc_m7</b>	T21	Equivalent of compo_fc for HAMM7

These two tests allow us to separate the test of our HAMM7 implementation in two phases: without interaction with radiation scheme; with explicit interaction with radiation scheme (ecrad). In the case of 'compo\_fc\_climrad', the radiation is processing considering climatological aerosols while the rest of the code is using HAMM7 parametrization. At this stage the hybrid-aerosols scheme with HAMM7 only considers a full climatological or a full prognostics approach.

To only run the specific ifs-tests we can proceed with **ifs-test -cvt -L m7** while the options: **-cb** can be run independently of any specific aerosol-scheme.

### 3.1.4 ifs-defaults

Default settings and switches for actual IFS experiments are defined as part of the ifs-defaults repository. As the aerosol scheme in the IFS has always been the 'AER' scheme, the default set of switches did not support an alternative scheme for the aerosol module. This is now changed, following the analogy for the chemistry module where three alternative schemes were always supported.

## 3.2 OpenIFS

Most of the HAMM7 development was first implemented in OpenIFS CY48R1. The implementation in the IFS code began before the implementation in OpenIFS was completed. A parallel, further development of OpenIFS took place, and the latest version of OpenIFS has additional developments that can be incorporated later in IFS as well. On the other side, IFS implementation has diverged as part of the code has been restructured/refactored and some abstractions have been added to simplify parts of the code. These differences are more obvious in `hamm7_interface.F90` and `m7_src_dust.F90`, but many files have been edited.

One important difference is the storage of optical properties calculated by HAMM7 modules used for the coupling with the ecRad radiation module. OpenIFS CY48R1 uses a custom derived type, but this causes friction with IFS CY49R1 code that was not present in CY48R1. For this reason, rather than a custom derived type, these optical properties are implemented in a standard data structure by adding a new object instance to the available grid-fields infrastructure of IFS. At this moment the respective part of the code and its full integration with ecRad is under testing.

## 4 Description of the HAMM7 modules

IFS-COMPO is a General Circulation Model (GCM) enhanced with modules that describe chemistry and aerosol processes. The default chemistry module is based on a modified version of the CB05 chemistry mechanism, coupled with stratospheric chemistry from the BASCOE module (ECMWF, 2024). The default aerosol module in CAMS is based on the AER scheme, but here we describe some of the main aspects of the newly introduced HAMM7 modules, as taken over from the implementation in OpenIFS CY48R1.

### 4.1 Microphysical core

The microphysical core of HAM is based on M7 (Vignati et al., 2004). It describes sulphate (SO<sub>4</sub>), black carbon (BC), organic aerosols (OA), sea salt and mineral dust using four water-soluble modes and three water-insoluble modes in different size ranges. In terms of dry particle diameters, the size ranges considered are 0–10 nm (nucleation mode), 10–100 nm (Aitken mode), 0.1–1 µm (accumulation mode) and >1 µm (coarse mode). The nucleation mode only exists for soluble particles, see Table 6.

**Table 6.** Aerosol tracers considered in this version of IFS-HAMM7

Short name	Long name	Short name	Long name
SO4_NS	Sulfate in wet nucleation mode	POM_KI	Organic matter in dry Aitken mode
SO4_KS	Sulfate in wet Aitken mode	POM_KS	Organic matter in wet Aitken mode
SO4_AS	Sulfate in wet accumulation mode	POM_AS	Organic matter in wet accumulation mode
SO4_CS	Sulfate in wet coarse mode	POM_CS	Organic matter in wet coarse mode
SS_AS	Sea salt in wet accumulation mode	NI_AS	Nitrate in wet accumulation mode
SS_CS	Sea salt in wet coarse mode	AM_AS	Ammonium in wet accumulation mode
DU_AI	Dust in dry accumulation mode	NS_N	Aerosol number in wet nucleation mode
DU_CI	Dust in dry coarse mode	KS_N	Aerosol number in wet Aitken mode
DU_AS	Dust in wet accumulation mode	AS_N	Aerosol number in wet accumulation mode
DU_CS	Dust in wet coarse mode	CS_N	Aerosol number in wet coarse mode
BC_KI	Black carbon in dry Aitken mode	KI_N	Aerosol number in dry Aitken mode
BC_KS	Black carbon in wet Aitken mode	AI_N	Aerosol number in dry accumulation mode
BC_AS	Black carbon in wet accumulation mode	CI_N	Aerosol number in dry coarse mode
BC_CS	Black carbon in wet coarse mode		

The particle size distribution in each mode is assumed to be a lognormal distribution with a fixed geometric standard deviation and variable geometric mean (median). The prognostic variables are the number of particles and the mass of each component contained in each mode.

The microphysical processes considered in M7 are nucleation, coagulation, sulfuric acid condensation and water uptake. Details on how these processes are described in M7 are given in Vignati et al. (2004). The new particle formation scheme of M7 has been modified following the approach of Bergman et al. (2022), introduced before in TM5 and EC-Earth3-AerChem (van Noije et al., 2021). This approach combines the parameterization from

Vehkamäki et al. (2002) for binary homogeneous water–sulfuric acid nucleation with a semi-empirical parameterization that produces enhanced nucleation rates in the presence of low-volatility oxidized organic vapours (Riccobono et al., 2014). Other aerosol processes including emission, secondary aerosol formation in the atmosphere, activation and cloud droplet formation, wet scavenging by clouds and precipitation, sedimentation and dry deposition, and heterogeneous chemistry on aerosol surfaces are not considered in M7. In the next subsections we briefly describe how these processes are represented in the new aerosol module.

The current implementation in IFS-COMPO does not yet include full parameterizations for secondary organic and inorganic aerosol, even though separate tracers for those components have already been prepared. While the activation of modules to describe secondary inorganic aerosol is subject of D3.2 in this project, the integration of secondary organic aerosol is planned for later.

## 4.2 Aerosol emissions

We use the default CAMS emissions (CAMS-GLOB-ANT v6.2; CAMS-GLOB-BIO v3.1; GFASv1.2) for the anthropogenic, biogenic and fire emissions, respectively.

Different to the bulk AER scheme, we now allow for a detailed specification of the size distribution of the aerosol sectoral emissions. Specifically, for each emission sector the specified bulk mass emissions for each component are distributed over the relevant modes and, for each of those modes, the corresponding particle number emissions are calculated based on an assumed mean or median particle diameter.

Emissions of sea salt and mineral dust are calculated online. Two distinct emission routines are available for calculating the emissions of sea salt, based on either TM5 or HAM. Both provide different options to describe the size distribution and dependence on wind speed and sea surface temperature (SST). The default sea salt emissions in the current implementation are based on Gong (2003) but with an additional SST dependence, with the temperature dependence taken from Sofiev et al. (2011).

The representation of mineral dust is based on the AER module (Remy et al., 2019), or Morcrette et al (2009), which, in turn, is based on Ginoux et al. (2001). Both dust schemes follow an empirical approach and consider a dust-source dependent calibration, which is suited for forecasting operations. The dynamics of the emission is considering the sandblasting approach present in Marticorena and Bergametti (1995) with wind velocity fields with updated turbulence. In our current test experiments the Morcrette et al. (2009) parameterization is used.

## 4.3 Aerosol removal processes

The HAMM7 module implemented in IFS-COMPO accounts for size-dependent in-cloud nucleation and impaction scavenging following the approach of Croft et al. (2010) as well as size-dependent below-cloud scavenging by rain and snow following Croft et al. (2009). The in-cloud scavenging scheme distinguishes between stratiform and convective clouds and warm, cold and mixed-phase clouds.

Modules for the calculation of aerosol dry deposition and sedimentation in IFS-COMPO have been taken over from the HAM implementation. Dry deposition is described using a standard resistance approach, where the deposition velocity is determined by the aerodynamic and surface resistances calculated for different surface types following Zhang et al. (2012). The

surface resistances depend on the size and density of the particles. In the model, the size dependence is accounted for by using the surface resistance values at the mode number median and mass mean diameter for deposition of particle number and mass, respectively. The dry deposition calculation is described in detail in a Technical Note by Kerckweg et al. (2006).

Sedimentation is applied to particles in the accumulation and coarse modes only. Settling velocities for particle number and mass are calculated following Zhang et al. (2012). The M7 sedimentation scheme implemented in IFS-COMPO provides the option to switch between an explicit and an implicit solver. The current default is to use the implicit solver as also adopted for the AER scheme (Rémy et al., 2019).

#### 4.4 Aerosol optical properties

The HAMM7 aerosol optical properties include the extinction cross section, single-scattering albedo, and asymmetry factor, each calculated for the specific wavelengths. The wavelengths selected here are the ones that are used in the IFS radiation scheme at 14 shortwave wavelength bands. There are two options for calculating these optical properties: the TM5 scheme from EC-Earth3-AerChem and a new scheme from HAMM7, with the latter now set as the default. The HAMM7 scheme also calculates these properties for 16 longwave wavelengths.

The TM5-scheme allows different aerosol species to be either externally or internally mixed. For the internally mixed modes, the model dynamically computes the effective refractive index by use of effective medium theory (EMT), employing either the Maxwell-Garnett or the Bruggeman mixing rule. EMT requires as input the volume fractions of the components in each of the mixed modes, as well as the spectrally dependent complex refractive indices from each of the chemical species contributing to the mixture. The latter are listed in Zhang et al. (2012).

For each mode the median effective particle diameter is computed. A look-up table is constructed with precomputed spectral optical properties for an adequate number of effective diameters and effective refractive indices, from which the extinction cross section, single-scattering albedo, and asymmetry parameter of each mode can be obtained. The optical properties averaged over the entire particle ensemble is then computed online by averaging optical properties over the seven modes.

In a future step the HAMM7 aerosol modes will be coupled to the radiation scheme through their optical properties, as already done in OpenIFS Cy48R1. As explained in section 3.2 this will introduce a difference at the level of the data-structure used for the implementation, while all other aspects remain identical. Also, special treatment for optical properties of stratospheric aerosol will then be considered. Additional work is ongoing to introduce modules that describe the activation of aerosol to form cloud droplets, but this is beyond the scope of the current efforts.

## 5 Verification

We have set up a model experiment for the period December 2018, and verify the model performance against a corresponding IFS-AER configuration. Both are run with the same ifs-source branch (nk9\_CY49R1.1\_m7dev\_v1c), and with essentially the same input emissions as described above. The model is run on T255 horizontal resolution ( $\sim 0.7^\circ$ ) with 137 model levels. While IFS-AER is initialized from a prior IFS-COMPO experiment with enabled aerosol dynamics, the IFS-HAMM7 starts from zero aerosol initialization, implying that the model spinup should be considered.

In this report we analyse two IFS-HAMM7 experiments: a version 'v0' and an updated version 'v1', which differ in their handling of various emissions, as specified below. They are compared against a default IFS-AER experiment for CY49R1, see also Table 7.

**Table 7.** Experiments considered in this report

Experiment	expid	Configuration
<b>IFS-AER</b>	b2qz	Reference IFS-AER experiment
<b>IFS-HAMM7-v0</b>	b2ri	First IFS-HAMM7 experiment assessed here
<b>IFS-HAMM7-v1</b>	b2ro	revised IFS-HAMM7 experiment with alternative settings for emissions

With regard to the differences between IFS-HAMM7 versions v0 and v1, we note the following:

### Dust emissions:

Compared to v0, v1 has updated (debugged) the conversion from dust mass to dust particle number, which results in a factor  $1e3$  higher emissions in terms of particle number (and consequently smaller particles), in line with a more recent version of OpenIFS.

### Sea salt emissions:

The temperature dependence in v1 has been updated to use the  $20^\circ\text{C}$  reference temperature instead of the  $15^\circ\text{C}$  (v0), to align with the default setting in OpenIFS.

### Fire OC and BC emissions:

To align with the AER implementation, in v1 we have added a scaling factor of 1.5 for fire BC and OC emissions. This was motivated by a general under-estimate in IFS-AER, compared to observed AOD for fire-affected aerosol, and attributed to missing (precursor) emissions. Note that in earlier versions of IFS-AER, which did not include a parameterization of secondary organic aerosol and different optics for OM, this factor was set to 3.4.

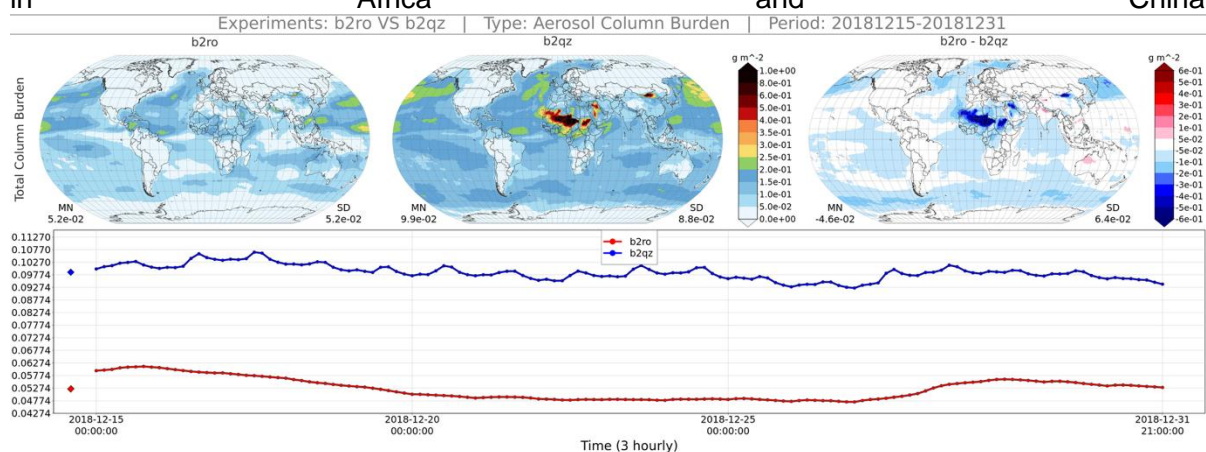
### Anthropogenic and fire OC emissions:

IFS-AER includes an additional 1.8 scale factor to convert prescribed OC emissions into OM for anthropogenic as well as fire emissions. From literature, a range of values is suggested of about 1.4 – 2.3, i.e. this scaling is not specific to IFS-AER. On the other hand, so far in IFS-HAMM7 no such conversion had been adopted. Here we test this upscaling using a factor 1.8 also in 'v1'. The default setting for HAMM7 in the scope of OpenIFS is a value of 1.6, with a distribution over different OM aerosol types.

Note that while the changes in the sea salt and dust emissions concern code changes in ifs-source, the changes in the scaling factors for fire and OM emissions are handled by the emission specification file. For this, a new version (v1.1) was created for expid b2rn as a copy of emission spec. file v1 used in expid b2ri.

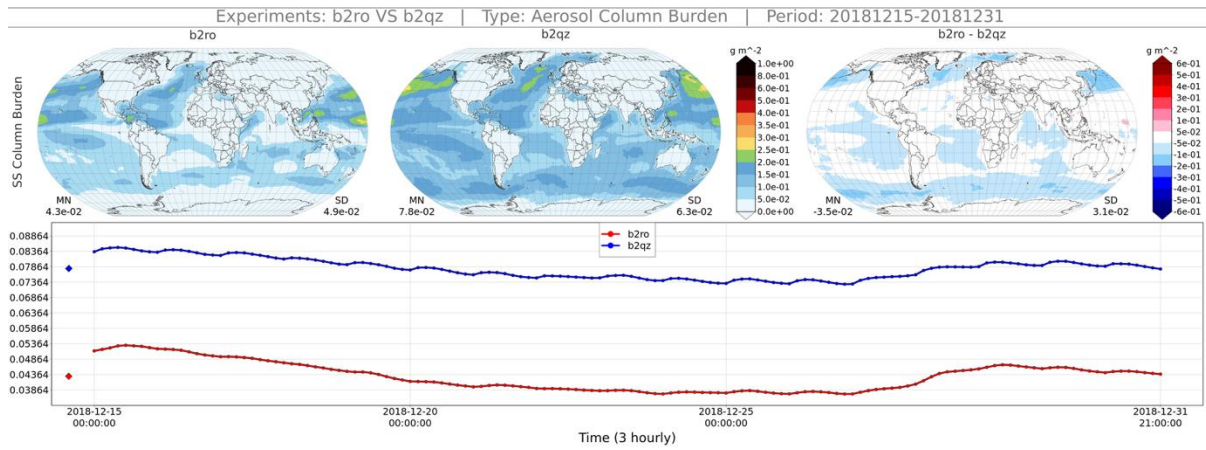
## 5.1 Comparison of total columns

In this section we present distributions of the average aerosol total column burden for December 2018 for experiment HAMM7-v1 as compared to IFS-AER, along with its differences and the time evolution. This gives a first impression of specifics of the current IFS-HAMM7 implementation. For this comparison, the contribution of bins (for IFS-AER) and modes (IFS-HAMM7-v1) are summed for the different aerosol types, to allow a quick, basic assessment. Note that b2ro aerosol fields (column burden, deposition, optical properties) are not initialized from a spin-up simulation, hence all aerosol fields are low and still increase during the first week. Here we show the model fields for the last two weeks of December 2018, i.e. allowing for a short, 14-day spinup period. Figure 1 shows the total burden of all aerosol types added together. Whereas the total mass over the oceans in IFS-HAMM7-v1 appears in line with IFS-AER, over land total column burden is lower over the desert dust source regions in Africa and China.



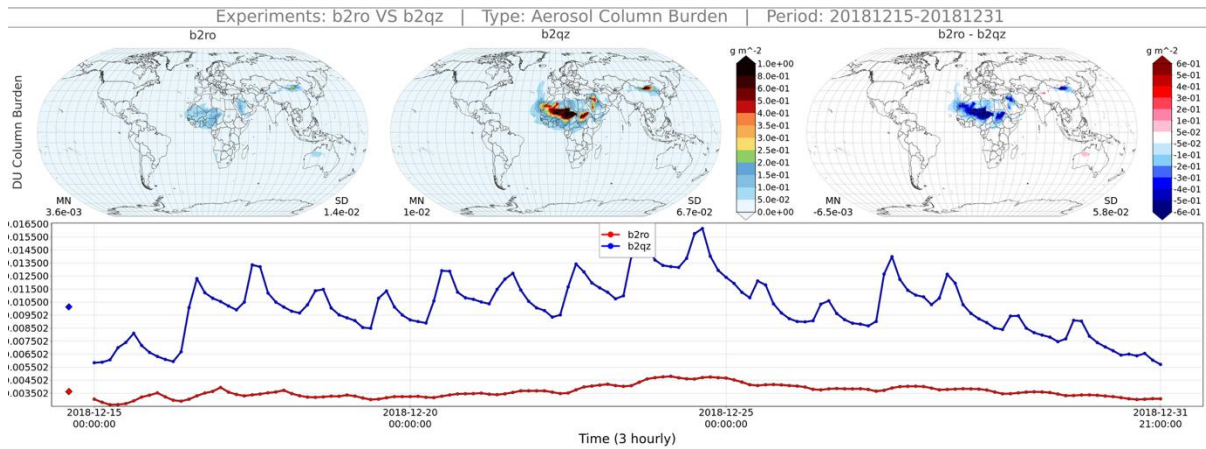
**Figure 1.** Total aerosol burden for IFS-HAMM7-v1 (left), IFS-AER (middle), their difference (HAMM7-AER) (right column) for the period 15-31 December 2018, and its global mean time evolution (bottom). Red (b2ro): IFS-HAMM7 and blue (b2qz): IFS-AER.

This is confirmed in Figure 2, which compares the contribution of sea salt aerosol between IFS-HAMM7 and IFS-AER. As a global average IFS-AER sea salt aerosol ranges around  $0.08 \text{ g m}^{-2}$ , while in IFS-HAMM7 the sea salt aerosol ranges around  $0.04 \text{ g m}^{-2}$ . Still, the patterns of high columns are mostly similar.



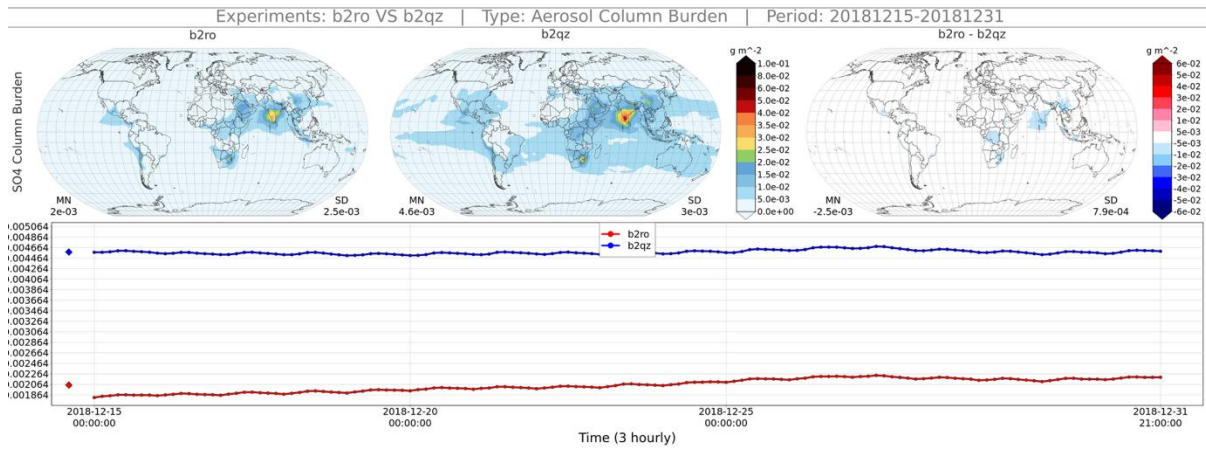
**Figure 2.** Sea salt aerosol burden for IFS-HAMM7-v1 (left), IFS-AER (middle), their difference (HAMM7-AER) (right column), for the period 15-31 December 2018, and its global mean time evolution (bottom). Red (b2ro): IFS-HAMM7 and blue (b2qz): IFS-AER.

Figure 3 shows a map of differences in dust aerosol between IFS-HAMM7 and IFS-AER. Overall, the same source regions with elevated dust levels show up in IFS-HAMM7 compared to IFS-AER, but the magnitude in IFS-HAMM7 is still about a factor 2-3 lower than IFS-AER. Also the diurnal cycle is much weaker in IFS-HAMM7.



**Figure 3.** Desert dust burden for IFS-HAMM7-v1 (left), IFS-AER (middle), their difference (HAMM7-AER) (right column), for the period 15-31 December 2018, and its global mean time evolution (bottom). Red (b2ro): IFS-HAMM7 and blue (b2qz): IFS-AER.

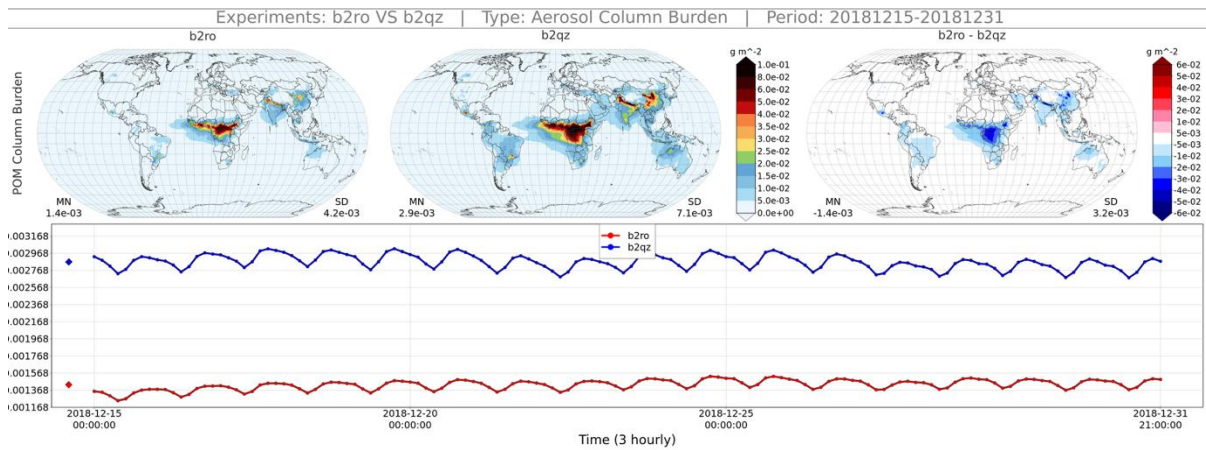
Figure 4 compares the sulphate burden for IFS-HAMM7 against IFS-AER. As for the dust aerosol, the source regions are very similar, but values, markedly at background locations, but also over the large source region over India, are significantly lower than IFS-AER.



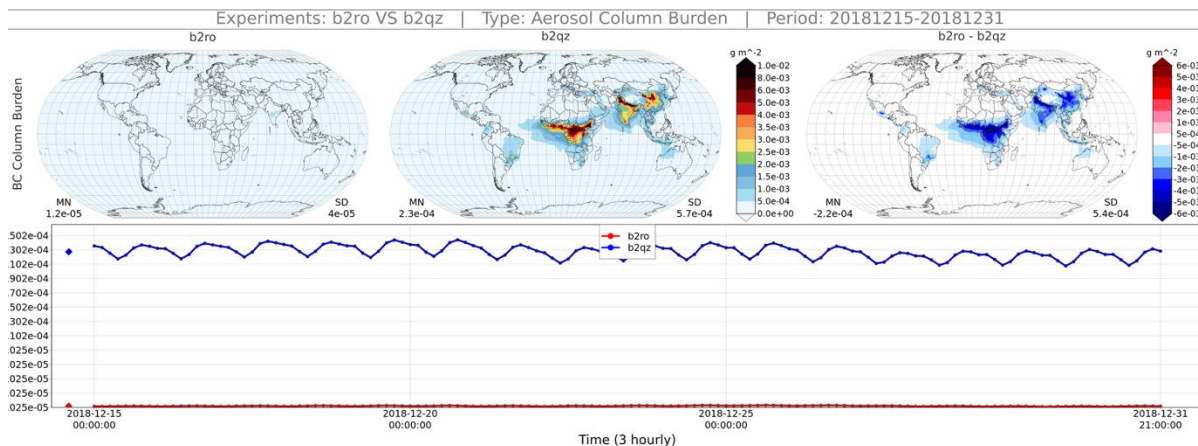
**Figure 4.** Sulphate burden for IFS-HAMM7-v1 (left), IFS-AER (middle), their difference (HAMM7-AER) (right column), for the period 15-31 December 2018, and its global mean time evolution (bottom). Red (b2ro): IFS-HAMM7 and blue (b2qz): IFS-AER.

Figure 5 presents the primary organic matter burden for IFS-HAMM7 against IFS-AER. Again, the values are lower in IFS-HAMM7 compared to IFS-AER, but the spatial distribution is similar. Finally, Figure 6 presents the distribution of black carbon. While values range up to 0.01 g m<sup>-2</sup> locally in IFS-AER, for IFS-HAMM7 they do not exceed a value of 0.001 g m<sup>-2</sup>, indicating a large inconsistency in the treatment of black carbon.

A further assessment of the causes of these communalities and differences is given in the next section.



**Figure 5.** Organic matter burden for IFS-HAMM7-v1 (left), IFS-AER (middle), their difference (HAMM7-AER) (right column), for the period 15-31 December 2018, and its global mean time evolution (bottom). Red (b2ro): IFS-HAMM7 and blue (b2qz): IFS-AER.



**Figure 6.** Black carbon burden for IFS-HAMM7-v1 (left), IFS-AER (middle), their difference (HAMM7-AER) (right column), for the period 15-31 December 2018, and its global mean time evolution (bottom). Red (b2ro): IFS-HAMM7 and blue (b2qz): IFS-AER.

## 5.2 Mass diagnostics

We analyse the mass diagnostics from the two IFS-HAMM7 experiments, and compare this to IFS-AER, see Tables 8-12. For this, we use the last 11 days in December 2018, i.e. after a 20-day spin-up period. We realize that this spin-up is short, and the 11-day period that is assessed is very short to make quantitative statements on annual total budgets. The lifetimes in the tables are computed by dividing the loss due to dry and wet deposition and sedimentation by the tropospheric burden. For now, this ignores the lifetime due to microphysics, as this term is currently not available from the budget output. Despite these limitations, this analysis is sufficient for the purpose here, which is to verify the implementation, and assess how IFS-HAMM7 burdens and tendencies currently relate to those in IFS-AER. The 11-day totals are converted into annual total numbers by scaling with a factor [365/11], just to make the numbers more comparable to reported values in literature. A difference between IFS-AER and IFS-HAMM7 is that sedimentation is accounted for in the dry deposition diagnostic with IFS-AER while it is a separated diagnostic for IFS-HAMM7.

**Table 8.** production and loss budgets for sea salt aerosol in the various experiments and for the various aerosol types. Units are in [Tg/yr] unless indicated differently

Sea salt Aerosol type	HAMM7-v0 AS / CS	HAMM7-v1 AS / CS	AER Bins 1 / 2 / 3
Emission	7.6 / 1.7e4	9.0/2.0e4	3e2 / 1e4 /3.6e5
Net microphys. prod./loss	-	-	-
dry deposition	0.5 / 2.4e3	0.6 / 2.8e3	1e2 / 6.6e3 /3.3e4
wet deposition	7.0 / 7.6e3	8.2 / 9.0e3	2e2 / 3.1e3 / 2.7e3
sedimentation	- / 7.2e3	- / 8.5e3	- / - / -
trop. burden [Tg]	4e-2 / 21	5e-2 / 26	2.1 / 22 / 17
lifetime [days]	1.9 / 0.46	1.9 / 0.46	2.2 / 0.8 / 0.18

Budgets of sea salt (Table 8) show a rather different distribution of emissions over the different aerosol tracers in HAMM7 as compared to AER, associated to the different aerosol size distribution handling. Whereas AER also has a very coarse aerosol type, this is missing in HAMM7, but it's impact on AOD is expected minor. The aerosol lifetime is rather comparable between HAMM7 and AER. HAMM7-v1 shows about 15% larger emissions than HAMM7-v0, which translates into an equally higher burden. The origin of the differences requires further analysis.

Desert dust (Table 9) also shows a rather different distribution of emissions over the different aerosol tracers in HAMM7 as compared to AER, again associated to the different aerosol size distribution handling as well as different assumptions about the size distribution of desert dust emissions. Also, here the total emissions are lower, due to the large (mass) emissions in Bin 3 in AER, the coarsest aerosol type, which has a much higher cutoff size than the coarse mode of IFS-HAMM7 (20 micron radius versus 10 micron diameter). Again, it's impact on AOD is expected minor. The aerosol lifetime varies between the aerosol types, and between HAMM7 and AER, but should be considered with care considering the non-negligible microphysics production/loss, not accounted here. HAMM7-v1 shows identical total emissions in mass as v0, but the loss terms are very different, with lower loss rates overall. This is due to the different (higher) particle number emissions, causing smaller particles.

This translates into higher burden, and overall increased lifetimes in HAMM7-v1, which brings them closer in line with AER, when excluding the mass in Bin 3.

**Table 9.** Production and loss budgets for desert dust aerosol in the various experiments and for the various aerosol types. Units are in [Tg/yr] unless indicated differently

Desert dust Aerosol type	HAMM7-v0 AI / AS / CI / CS	HAMM7-v1 AI / AS / CI / CS	AER Bins 1 / 2 / 3
Emission	49 / - / 97 / -	49 / - / 97 / -	3.5 / 31 / 2.2e3
Net microphys. prod./loss	-13 / 13 / -2.2 / 2.3	-43 / 43 / -43 / 43	-
dry deposition	6.0 / 1.1 / 37 / 0.3	2 / 3.7 / 6.7 / 3.8	1.5 / 15 / 2.2e3
wet deposition	2.2 / 10.5 / 0.5 / 0.8	4.5 / 34 / 11 / 20	1.7 / 16 / 1e2
sedimentation	29 / - / 58 / 1.2	0.9 / 0.3 / 42 / 17	-
trop. burden [Tg]	0.1 / 0.2 / 0.05 / 0.02	0.35 / 0.8 / 0.6 / 0.4	0.06 / 0.6 / 5.0
lifetime [days]	1.4 / 7.5 / 0.2 / 3.0	17 / 7.3 / 3.8 / 3.4	7.0 / 6.5 / 0.8

There is again a large difference in the treatment of sulphate aerosol between IFS-AER (only a single tracer) and IFS-HAMM7 (4 tracers, in addition to an explicit treatment of H<sub>2</sub>SO<sub>4</sub> also in the troposphere), see Table 10. The total production budget matches very well between IFS-HAMM7 and IFS-AER. The largest amount of mass is in the Accumulation Soluble mode (AS), which dominates the overall budget and is most easily compared between IFS-HAMM7 and IFS-AER. Still, the total tropospheric burden for sulphate is lower in IFS-HAMM7 (~1.2 Tg) than IFS-AER (~1.9 Tg), associated to a more efficient loss due to wet deposition.

As there is no change in the treatment of SO<sub>2</sub> precursor emissions between HAMM7-v0 and HAMM7-v1, the changes in the sulphate budgets are overall smaller.

**Table 10.** Production and loss budgets for sulphate in the various experiments and for the various aerosol types. Units are in [Tg/yr] unless indicated differently

Sulphate Aerosol type	HAMM7-v0 NS / KS / AS / CS	HAMM7-v1 NS / KS / AS / CS	AER
Emission	-	-	-
Net microphys. prod./loss	0 / 1.7 / 130 / 9	0 / 1.7 / 125 / 9.0	139
dry deposition	0 / 0.2 / 4.7 / 0.4	0 / 0.16 / 5 / 0.4	18
wet deposition	3e-3 / 2.3 / 119 / 6.7	3e-3 / 1.9 / 115 / 6.6	119
sedimentation	- / 0.2 / 1.9	- / - / 0.2 / 1.9	-
trop. burden [Tg]	1e-3 / 0.13 / 1.1 / 0.03	1e-3 / 0.1 / 1.1 / 0.03	1.9
lifetime [days]	- / 19 / 3.3 / 1.1	- / 19 / 3.5 / 1.2	5.1

Table 11 shows a comparison of the budgets for primary organic matter. Compared to IFS-AER, the total emissions are well matched in HAMM7-v1, while they are a factor 2 lower in HAMM7-v0. All the other budget tendencies scale with these differences. The largest amount of mass in HAMM7-v1 is in the Accumulation Soluble mode (0.1 Tg), which is still about a factor 10 lower in the hydrophilic component of organic matter in IFS-AER (1.0 Tg). These differences likely point to a higher wet removal efficiency in IFS-HAMM7 than IFS-AER, quantified by a lower lifetime (5.4 days for the Accumulation Soluble mode for HAMM7-v1, compared to 7 days for IFS-AER)

**Table 11.** Production and loss budgets for organic matter aerosol in the various experiments and for the various aerosol types. Units are in [Tg/yr] unless indicated differently.

Organic Matter Aerosol type	HAMM7-v0 KI / KS / AS / CS	HAMM7-v1 KI / KS / AS / CS	AER OM-phob / OM-phil
Emission	24 / - / - / -	52 / - / - / -	26 / 26
Net microphys. prod./loss	-22 / 1.2 / 21 / 0.03	-48 / 1.5 / 46 / 0.06	-25 / 25
dry deposition	1.5 / 0.2 / 1.7 / 2e-3	3.1 / 0.3 / 3.7 / 4e-3	1.1 / 11
wet deposition	0.64 / 1 / 18 / 0.02	1.5 / 1.3 / 41 / 0.04	0.02 / 41
sedimentation	- / - / - / 0.01	- / - / - / 0.02	
trop. burden [Tg]	0.04 / 0.03 / 0.3 / 2e-4	0.1 / 0.05 / 0.1 / 4e-4	1e-2 / 1.0
lifetime [days]	7.6 / 9.1 / 5.0 / 1.8	9.0 / 10 / 5.4 / 2.1	3.1 / 7.0

Finally, Table 12 shows a comparison of the budgets for black carbon. Even though total emissions are comparable between IFS-AER and IFS-HAMM7, the other terms in the budget calculation are still very different. The total emissions in HAMM7-v1 are a bit higher than those in HAMM7-v0, but not sufficient to help explain the differences with IFS-AER.

In general, when adding up all the loss terms in the IFS-HAMM7 experiments, this does not match up with the total emissions, suggesting a problem with the conversion of black carbon in the microphysics scheme as implemented in IFS. This causes significantly lower total tropospheric burden (order 0.01 Tg) in IFS-HAMM7 compared to IFS-AER (order 0.1 Tg).

**Table 12.** production and loss budgets for black carbon aerosol in the various experiments and for the various aerosol types. Units are in [Tg/yr] unless indicated differently

Black Carbon Aerosol type	HAMM7-v0 KI / KS / AS / CS	HAMM7-v1 KI / KS / AS / CS	AER BC-B / BC-A
Emission	6.4 / - / - / -	7.0 / - / - / -	5.7 / 1.4
Net microphys. prod./loss	- / 0.03 / 0.7 / 9e-4	- / 0.02 / 0.6 / 7e-4	-5.4 / 5.4
dry deposition	0.06 / 0.01 / 0.07	0.06 / 0.07 / 0.06 / 1e-4	0.2 / 1.5
wet deposition	- / 0.02 / 0.6	0 / 0.1 / 0.5	4-e3 / 5.4
sedimentation	- / - / 2e-3 / -	- / - / 2e-3 / -	- / -
trop. burden [Tg]	0 / 4e-4 / 9e-3 / 0	0 / 3e-4 / 8e-3 / 0	2e-3 / 0.1
lifetime [days]	0 / 6.0 / 4.9 / 1.8	0 / 6.0 / 5.0 / 2.0	3.2 / 6.1

### 5.3 Comparison of AOD

In this section we compare aspects related to the optical properties in IFS-HAMM7-v1 compared to IFS-AER. To some extent in contrast with the previous sections, the AOD is on average higher in IFS-HAMM7 than in IFS-AER, with varying contributions from the different aerosol types. While over the oceans (dominated by sea salt) the differences in AOD for IFS-HAMM7-v1 compared to IFS-AER are on the order of +0.2, this is negative over regions dominated by biomass burning (central Africa, southeast Asia: -0.2). Over regions with strong anthropogenic pollution (India, China) IFS-HAMM7 shows a positive difference of up to 0.4. The absorption component of AOD (Figure 8) is severely lower in IFS-HAMM7 than IFS-AER. Whereas AAOD values range up to 0.1 in IFS-AER, they only go up to 0.01 in IFS-HAMM7, which can be understood in terms of correspondingly high differences in the tropospheric burden of black carbon.

Finally, the Mass Extinction Coefficient (MEC), which is a metric that describes the contribution to AOD per kg total aerosol mass, shows rather large differences as well. MEC for IFS-HAMM7 is generally much higher in IFS-HAMM7 than IFS-AER, but especially over the continents driven by anthropogenic pollution. This suggests that the average aerosol type (mostly due to OM) is optically more thick in IFS-HAMM7 than IFS-AER, requiring less aerosol to achieve the same level of AOD.

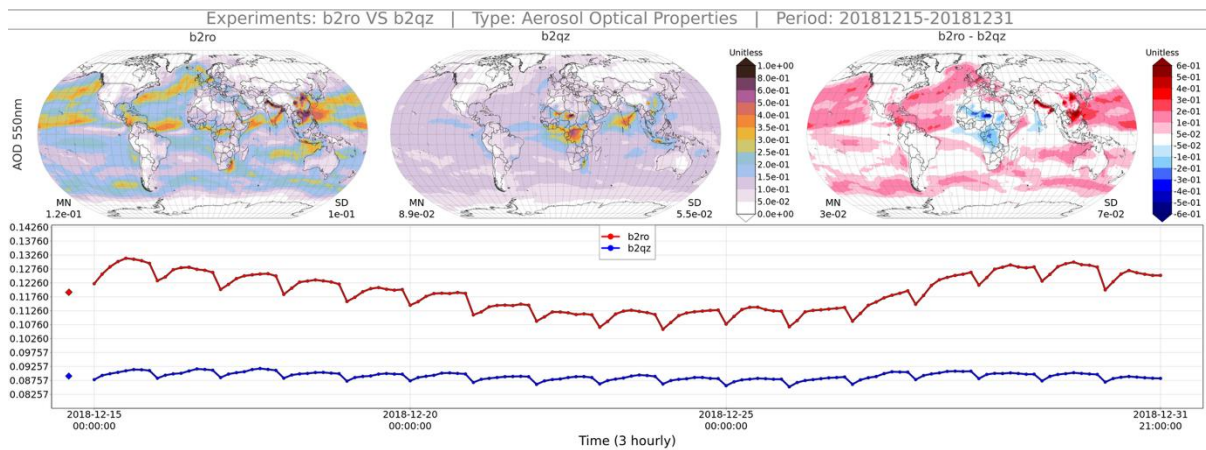


**Figure 7.** Monthly average AOD at 550 nm in IFS-HAMM7-v1 (left), IFS-AER (middle), their difference (HAMM7-AER) (right), for the period 15-31 December 2018, and its global mean time evolution (bottom). Red (b2ro): IFS-HAMM7 and blue (b2qz): IFS-AER.

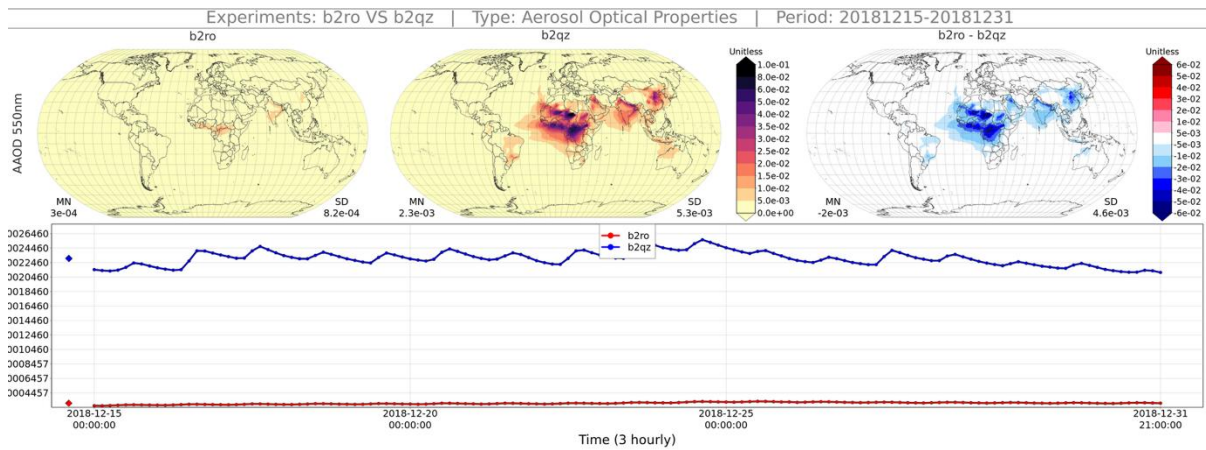


**Figure 8.** Monthly average absorption AOD at 550 nm in IFS-HAMM7-v1 (left), IFS-AER (middle), their difference (HAMM7-AER) (right), for the period 15-31 December 2018, and its global mean time evolution (bottom). Red (b2ro): IFS-HAMM7 and blue (b2qz): IFS-AER.

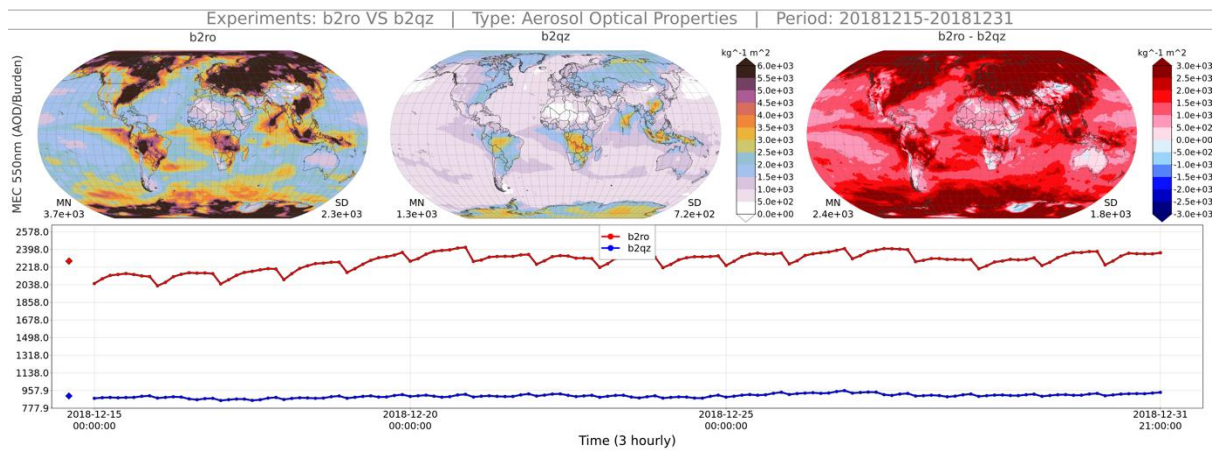


**Figure 9.** Mass extinction coefficient (MEC, AOD divided by burden, in units  $\text{kg}^{-1} \text{m}^{-2}$ ) at 550 nm in IFS-HAMM7-v1 (left), IFS-AER (middle), their difference (HAMM7-AER) (right), for the period 15-31 December 2018, and its global mean time evolution (bottom). Red (b2ro): IFS-HAMM7 and blue (b2qz): IFS-AER.

## 6 Conclusion

In this document we have described a first technical implementation of M7 aerosols module into CY49R1 of the IFS based on the HAMM7 code that was earlier implemented in OpenIFS. This required modifications of various parts of the code and script repositories that come with the IFS, along with selection and preparation of the input data. The largest modifications were in the ifs-source repository.

We successfully simulated HAMM7 aerosol emissions, transport, conversion, dry and wet deposition, sedimentation, for the aerosol tracers which represent sea salt, desert dust, sulphate, organic matter and black carbon. Secondary inorganic aerosol from other sources (nitrate and ammonium) has been introduced in parallel; this is the subject of a second Deliverable report (D3.2), while the secondary organic aerosol is not yet considered here. Also, the feedback of aerosol to chemistry (heterogeneous loss and optics), and meteorology (optics) is not yet in place.

We diagnosed the distribution of aerosol burden, its tendencies, and the optical properties through AOD, AAOD and MEC. In particular, we compared two configurations of IFS-HAMM7, which differed in their specification of emissions, and compared this to a default configuration of IFS-AER. The spinup-time was very short, but still sufficient to identify the major features of the current implementation of IFS-HAMM7.

While both IFS-HAMM7 versions show correct reproduction of the spatial distribution of the aerosol types, the version with enhanced emissions shows the best performance. Still overall the computed tropospheric burdens are significantly lower than those computed with IFS-AER. On the other hand, the AOD was similar or higher in IFS-HAMM7 compared to IFS-AER, suggesting quite different optical properties of the various aerosol types. Looking at absorption AOD, and at the black carbon contribution specifically, shows that there is still an issue with the tracers and microphysics involved here.

Furthermore, it appears that the lifetime of the aerosol tracers in IFS-HAMM7 is lower than those in IFS-AER, which can mainly be attributed to more efficient wet removal.

### Outlook

During the second phase of the CAMAERA project we will put efforts on the following subjects.

From a coding perspective, many parts of the code require further scrutiny regarding the following aspects:

- Code in the HAMM7\_INTERFACE routine needs to be broken up in more individual subroutines, with clear interfaces. This should support the readability as well as the model stability.
- Updates done in OpenIFS need to be ported towards IFS CY49R1, such as an updated parameterisation of sea salt emissions.
- Flags used to activate different settings in the IFS-HAMM7 code need to be checked and aligned, where feasible, with IFS-AER. Ideally this comes with a further harmonisation of routines for describing emissions (and deposition) between IFS-AER and IFS-HAMM7.
- Migration of the model code towards more recent cycle, and back-porting relevant code changes to OpenIFS, to make this available to EC-Earth as well.

From a parameterization implementation and evaluation perspective the following activities will take place:

- Further integration of couplings between IFS-HAMM7 aerosol and the rest of the system, including secondary organic and inorganic aerosol, heterogeneous chemistry, stratospheric chemistry, photolysis and radiation.
- Further analysis of differences between IFS-AER and IFS-HAMM7, and optimization of the IFS-HAMM7 model performance through targeted assessments of processes and parameterizations.

While many of these aspects are the subject of the second phase of the CAMAERA project, some of these are also considered in sister research projects (FOCI: support for EC-Earth) and/or covered in CAMS more operational support activities (CAMS2\_35\_bis: migration towards newer cycles).

## References

Abdul-Razzak, H. and Ghan, S. J.: A parameterization of aerosol activation: 2. Multiple aerosol types, *J. Geophys. Res.*, 105, 6837–6844, <https://doi.org/10.1029/1999JD901161>, 2000.

Bergman, T., Makkonen, R., Schrödner, R., Swietlicki, E., Phillips, V. T. J., Le Sager, P., and van Noije, T.: Description and evaluation of a secondary organic aerosol and new particle formation scheme within TM5-MP v1.2, *Geosci. Model Dev.*, 15, 683–713, <https://doi.org/10.5194/gmd-15-683-2022>, 2022.

Croft, B., Lohmann, U., Martin, R. V., Stier, P., Wurzler, S., Feichter, J., Posselt, R., and Ferrachat, S.: Aerosol size-dependent below-cloud scavenging by rain and snow in the ECHAM5-HAM, *Atmos. Chem. Phys.*, 9, 4653–4675, <https://doi.org/10.5194/acp-9-4653-2009>, 2009.

Croft, B., Lohmann, U., Martin, R. V., Stier, P., Wurzler, S., Feichter, J., Hoose, C., Heikkilä, U., van Donkelaar, A., and Ferrachat, S.: Influences of in-cloud aerosol scavenging parameterizations on aerosol concentrations and wet deposition in ECHAM5-HAM, *Atmos. Chem. Phys.*, 10, 1511–1543, <https://doi.org/10.5194/acp-10-1511-2010>, 2010.

ECMWF: IFS Documentation CY49R1 – Part VIII: Atmospheric composition, ECMWF, <https://doi.org/10.21957/d13af18259>, 2024.

Ginoux, P., Chin, M., Tegen, I., Prospero, J. M., Holben, B., Dubovik, O., & Lin, S. J.: Sources and distributions of dust aerosols simulated with the GOCART model. *Journal of Geophysical Research: Atmospheres*, 106(D17), 20255–20273, 2001.

Gong, S. L.: A parameterization of sea-salt aerosol source function for sub- and super-micron particles, *Global Biogeochem. Cy.*, 17, 1097, <https://doi.org/10.1029/2003GB002079>, 2003.

Huijnen, V., Le Sager, P., Köhler, M. O., Carver, G., Rémy, S., Flemming, J., Chabrilat, S., Errera, Q., and van Noije, T.: OpenIFS/AC: atmospheric chemistry and aerosol in OpenIFS 43r3, *Geosci. Model Dev.*, 15, 6221–6241, <https://doi.org/10.5194/gmd-15-6221-2022>, 2022.

Kerkweg, A., Buchholz, J., Ganzeveld, L., Pozzer, A., Tost, H., and Jöckel, P.: Technical Note: An implementation of the dry removal processes DRY DEPosition and SEDImentation in the Modular Earth Submodel System (MESSy), *Atmos. Chem. Phys.*, 6, 4617–4632, <https://doi.org/10.5194/acp-6-4617-2006>, 2006.

Marticorena, B., and Bergametti, G.: Modeling the atmospheric dust cycle: 1. Design of a soil-derived dust emission scheme. *Journal of geophysical research: atmospheres*, 100(D8), 16415–16430, 1995.

Morales Betancourt, R. and Nenes, A.: Droplet activation parameterization: the population-splitting concept revisited, *Geosci. Model Dev.*, 7, 2345–2357, <https://doi.org/10.5194/gmd-7-2345-2014>, 2014.

Morcrette, J.-J., Boucher, O., Jones, L., Salmond, D., Bechtold, P., Beljaars, A., Benedetti, A., Bonet, A., Kaiser, J. W., Razinger, M., Schulz, M., Serrar, S., Simmons, A. J., Sofiev, M., Suttie, M., Tompkins, A. M., and Untch, A.: Aerosol analysis and forecast in the European Centre for Medium-Range Weather Forecasts Integrated Forecast System: Forward modeling, *J. Geophys. Res.*, 114, D06206, doi:10.1029/2008JD011235, 2009.

Rémy, S., Kipling, Z., Flemming, J., Boucher, O., Nabat, P., Michou, M., Bozzo, A., Ades, M., Huijnen, V., Benedetti, A., Engelen, R., Peuch, V.-H., and Morcrette, J.-J.: Description and evaluation of the tropospheric aerosol scheme in the European Centre for Medium-Range Weather Forecasts (ECMWF) Integrated Forecasting System (IFS-AER, cycle 45R1), *Geosci. Model Dev.*, 12, 4627–4659, <https://doi.org/10.5194/gmd-12-4627-2019>, 2019.

Rémy, S., Metzger, S., Huijnen, V., Williams, J. E., and Flemming, J.: An improved representation of aerosol in the ECMWF IFS-COMPO 49R1 through the integration of EQSAM4Climv12 – a first attempt at simulating aerosol acidity, *Geosci. Model Dev.*, 17, 7539–7567, <https://doi.org/10.5194/gmd-17-7539-2024>, 2024.

Riccobono F., Schobesberger S., Scott C. E., Dommen, J., Ortega, I. K., Rondo, L., Almeida, J., Amorim, A., Bianchi, F., Breitenlechner, M., David, A., Downard, A., Dunne, E. M., Duplissy, J., Ehrhart, S., Flagan, R. C., Franchin, A., Hansel, A., Junninen, H., Kajos, M., Keskinen, H., Kupc, A., Kürten, A., Kvashin, A. N., Laaksonen, A., Lehtipalo, K., Makhmutov, V., Mathot, S., Nieminen, T., Onnela, A., Petäjä, T., Praplan, A. P., Santos, F. D., Schallhart, S., Seinfeld, J. H., Sipilä, M., Spracklen, D. V., Stozhkov, Y., Stratmann, F., Tomé, A., Tsagkogeorgas, G., Vaattovaara, P., Viisanen, Y., Vrtala, A., Wagner, P. E., Weingartner, E., Wex, H., Wimmer, D., Carslaw, K. S., Curtius, J., Donahue, N. M., Kirkby, J., Kulmala, M., Worsnop, D. R., and Baltensperger, U.: Oxidation products of biogenic emissions contribute to nucleation of atmospheric particles, *Science*, 344, 717–721, <https://doi.org/10.1126/science.1243527>, 2014.

Salter, M. E., Zieger, P., Acosta Navarro, J. C., Grythe, H., Kirkevåg, A., Rosati, B., Riipinen, I., and Nilsson, E. D.: An empirically derived inorganic sea spray source function incorporating sea surface temperature, *Atmos. Chem. Phys.*, 15, 11047–11066, <https://doi.org/10.5194/acp-15-11047-2015>, 2015.

Sofiev, M., Soares, J., Prank, M., de Leeuw, G., and Kukkonen, J.: A regional-to-global model of emission and transport of sea salt particles in the atmosphere, *J. Geophys. Res.*, 116, D21302, <https://doi.org/10.1029/2010JD014713>, 2011.

Tegen, I., Neubauer, D., Ferrachat, S., Siegenthaler-Le Drian, C., Bey, I., Schutgens, N., Stier, P., Watson-Parris, D., Stanelle, T., Schmidt, H., Rast, S., Kokkola, H., Schultz, M., Schroeder, S., Daskalakis, N., Barthel, S., Heinold, B., and Lohmann, U.: The global aerosol–climate model ECHAM6.3–HAM2.3 – Part 1: Aerosol evaluation, *Geosci. Model Dev.*, 12, 1643–1677, <https://doi.org/10.5194/gmd-12-1643-2019>, 2019.

van Noije, T., Bergman, T., Le Sager, P., O'Donnell, D., Makkonen, R., Gonçalves-Ageitos, M., Döscher, R., Fladrich, U., von Hardenberg, J., Keskinen, J.-P., Korhonen, H., Laakso, A., Myriokefalitakis, S., Ollinaho, P., Pérez García-Pando, C., Reerink, T., Schrödner, R., Wyser, K., and Yang, S.: EC-Earth3-AerChem: a global climate model with interactive aerosols and atmospheric chemistry participating in CMIP6, *Geosci. Model Dev.*, 14, 5637–5668, <https://doi.org/10.5194/gmd-14-5637-2021>, 2021.

Van Noije, T., Wu, L., Le Sager, P., Huijnen, V., Bergman, T., Kokkola, H., Laakso, A., Jorba, O., Gonçalves-Ageitos, M., Chatziparaschos, M., Costa Surós, M., Gromov, S., Pozzer, A.: Model improvements for physico-chemical processes of non-CO<sub>2</sub> radiative forcers, FOCI Deliverable report D3.1, 2025.

Vehkamäki, H., Kulmala, M., Napari, I., Lehtinen, K. E. J., Timmreck, C., Noppel, M., and Laaksonen, A.: An improved parameterization for sulfuric acid–water nucleation rates for tropospheric and stratospheric conditions, *J. Geophys. Res.*, 107, 4622, <https://doi.org/10.1029/2002JD002184>, 2002.

Vignati, E., Wilson, J., and Stier, P.: M7: An efficient size-resolved aerosol microphysics module for large-scale aerosol transport models, *J. Geophys. Res.*, 109, D22202, <https://doi.org/10.1029/2003JD004485>, 2004.

Zhang, K., O'Donnell, D., Kazil, J., Stier, P., Kinne, S., Lohmann, U., Ferrachat, S., Croft, B., Quaas, J., Wan, H., Rast, S., and Feichter, J.: The global aerosol-climate model ECHAM-HAM, version 2: sensitivity to improvements in process representations, *Atmos. Chem. Phys.*, 12, 8911–8949, <https://doi.org/10.5194/acp-12-8911-2012>, 2012.

## Document History

Version	Author(s)	Date	Changes
1.0	V. Huijnen et al.	6 June 2025	Initial version
1.1	V. Huijnen et al.	20 June 2025	Revised version

## Internal Review History

Internal Reviewers	Date	Comments
M. Ades; M. Kahnert	14 June 2025	
P. Franke	18 June 2025	

This publication reflects the views only of the author, and the Commission cannot be held responsible for any use which may be made of the information contained therein.